

研究成果の刊行に関する一覧表  
書籍

著者氏名	論文タイトル名	書籍全体の編集者名	書籍名	出版社名	出版地	出版年	ページ
片桐秀樹	神経系による糖・エネルギー代謝の臓器間協調的調節と肥満・糖尿病	菅村和夫 佐竹正延	遺伝子医学MOOK 6号「シグナル伝達病を知るーその分子機序解明から新たな治療戦略まで」	メディカルドゥ	日本	2006	249-254
岡芳知, 春日雅人, 片桐秀樹, 門脇孝, 小林哲朗, 三家登喜夫, 松谷朗, 宮田哲, 山田祐一郎	作成委員	日本糖尿病学会	糖尿病専門医研修ガイドブック 改訂第3版	診断と治療社	日本	2006	
荻原健英、穴井元暢、片桐秀樹、浅野知一郎	糖尿病とインスリン抵抗性	松澤祐次、藤田敏郎、門脇孝	インスリン抵抗性	医学書院	日本	2006	34-40
山田哲也、片桐秀樹	エネルギー代謝の恒常性維持機構の解析における最近の進歩	金澤康徳、武谷雄二、関原久彦、山田信博	Annual Review 糖尿病・代謝・内分泌	中外医学社	日本	2007	83-89
Sei Yonezawa, Tomohiro Asai, Naoto Oku	Dorsal air sac model	Carolyn A St aton, Claire Lewis, Roy Bicknell	Angiogenesis Assays	John Wiley & Sons, Ltd	England	2006	229-238

雑誌

発表者氏名	論文タイトル名	発表誌名	巻号	ページ	出版年
M. Akamatsu, Y. Fujimoto, M. Kataoka, Y. Suda, S. Kusumoto, and K. Fukase	Synthesis of lipid A monosaccharide analogues containing acidic amino acid: Exploring the structural basis for the endotoxic and antagonistic activities	<i>Bioorganic &amp; Medicinal Chemistry</i>	14	6759-6777	2006
Y. Suda, Y. Kishimoto, T. Nishimura, S. Yamashita, M. Hamamatsu, A. Saito, M. Sato, M. Wakao	Sugar-immobilized gold nanoparticles (SGNP): Novel bioprobe for the on-site analysis of the oligosaccharide protein interactions	<i>Polymer Preprints</i>	47 (2)	156-157	2006
Errol S. Wijelath, S. Rahman, M. Namekata, J. Murray, T. Nishimura, Z. Mostafavi-Pour, Y. Patel, Y. Suda, M. J. Humphries, M. Sobel	Heparin-II Domain of Fibronectin Is a Vascular Endothelial Growth Factor-Binding Domain. Enhancement of VEGF Biological Activity by a Singular Growth Factor/Matrix Protein Synergism	<i>Circ Res.</i>	99 (8)	853-860	2006

発表者氏名	論文タイトル名	発表誌名	巻号	ページ	出版年
<u>Y. Suda</u> , A. Arano, Y. Fukui, S. Koshida, M. Wakao, T. Nishimura, S. Kusumoto, M. Sobel	Immobilization and Clustering of Structurally Defined Oligosaccharides for Sugar Chips: An Improved Method for Surface Plasmon Resonance Analysis of Protein-Carbohydrate Interactions	<i>Bioconjug Chem.</i>	17 (5)	1125-1135	2006
M. Hashimoto, K. Tawaratsumida, H. Kariya, A. Kiyohara, <u>Y. Suda</u> , F. Kirikae, T. Kirikae, and F. Gotz	Not Lipoteichoic Acid but Lipoproteins Appear to Be the Dominant Immunobiologically Active Compounds in <i>Staphylococcus Aureus</i>	<i>The Journal of Immunology</i>	177	3162-3169	2006
M. Kataoka, M. Hashimoto, <u>Y. Suda</u> , S. Kusumoto, and K. Fukase	Synthesis and Biological Activities of Biscarboxymethyl Lipid Analogs	<i>Heterocycles</i>	69	395-415	2006
隅田泰生	ヘパリンと血小板ならびにフォンビルブランド因子との相互作用解析からシュガーチップの開発へ	ドージンニュース	121	1-10	2006
<u>Doh-ura K.</u> , Tamura K, Karube Y, Naito M, Tsuruo T, Kataoka Y	Chelating compound, chrysoidine, is more effective in both anti-prion activity and brain endothelial permeability than quinacrine	<i>Cell. Mol. Neurobiol.</i>			in press
Fukuuchi T, <u>Doh-ura K.</u> , Yoshihara S, Ohta S	Metal complexes with superoxide dismutase-like activity as candidates for anti-prion drug	<i>Bioorg. Med. Chem. Lett.</i>	16	5982-5987	2006
Ishikawa K, Kudo Y, Nishida N, Suemoto T, Sawada T, Iwaki T, <u>Doh-ura K.</u>	Styrylbenzazole derivatives for imaging of prion plaques and treatment of transmissible spongiform encephalopathies	<i>J. Neurochem.</i>	99	198-205	2006
Sasaki K, <u>Doh-ura k.</u> , Ironside J, Mabbott N, Iwaki T	Clusterin expression in follicular dendritic cells associated with prion protein accumulation	<i>J. Pathol.</i>	209 (4)	484-91	2006
Wakisaka Y, Santa N, <u>Doh-ura K.</u> , Kitamoto T, Ibayashi S, Iida M, Iwaki T	Increased asymmetric pulvinar magnetic resonance imaging signals in Creutzfeldt-Jakob disease with florid plaques following a cadaveric dura mater graft	<i>Neuropathol.</i>	26	82-88	2006
Shintaku M, Yutani C, <u>Doh-ura K.</u>	Brain stem lesions in sporadic Creutzfeldt-Jakob disease: A histopathological and immunohistochemical study	<i>Neuropathol.</i>	26	43-49	2006

発表者氏名	論文タイトル名	発表誌名	巻号	ページ	出版年
Kawatake S, Nishimura Y, Sakaguchi S, Iwaki T, <u>Doh-ura K</u>	Surface plasmon resonance analysis for the screening of anti-prion compounds	<i>Biol. Pharm. Bull.</i>	29 (5)	927-932	2006
逆瀬川裕二、 <u>堂浦克美</u>	プリオン病の治療 _その現状と展望_	<i>Brain Medical</i>	18 (4)	365-370	2006
逆瀬川裕二、 <u>堂浦克美</u>	孤発性クロイツフェルトーヤコブ病と6種類のサブタイプ	<i>Medical Briefs in Brain &amp; Nerve</i>	15 (4)	5-6	2006
石川謙介、 <u>堂浦克美</u>	プリオンイメージングの試み	<i>Clinical Neuroscience</i>	24 (3)	313-316	2006
Yamada, T., Ishihara, H., Tamamura, A., Takahashi., R, Yamaguchi, S., Takei., D, Tokita, A., Satake, C., Tashiro, F., <b>Katagiri, H.</b> , Aburatani, H., Miyazaki, J-I., Oka, Y.	WFS1-deficiency enhances endoplasmic reticulum stress, triggers apoptotic pathway and impairs cell cycle progression specifically in pancreatic $\beta$ -cells.	<i>Hum Mol Genet.</i>	15	1600-1609	2006
Uno K, <b>Katagiri H</b> , Yamada T, Ishigaki Y, Ogihara T, Imai J, Hasegawa Y, Gao J, Kaneko K, Iwasaki H, Ishihara H, Sasano H, Inukai K, Mizuguchi H, Asano T, Shiota M, Nakazato M, Oka Y	Neuronal pathway from the liver modulates energy expenditure and systemic insulin sensitivity.	<i>Science</i>	312	1656-1659	2006
Imai, J , <b>Katagiri, H.</b> , Yamada, T , Ishigaki, Y , Ogihara, T , Uno, K , Hasegawa, Y , Gao, J , Ishihara, H , Oka, Y	Activation of sympathetic nervous system suppresses serum adiponectin levels in mice.	<i>Obesity</i>	14	1132-1141	2006
Takei, D., Ishihara, H., Yamaguchi, S., Yamada, T., <b>Katagiri, H.</b> , Maruyama, Y., Oka, Y	WFS1 protein modulates the free Ca <sup>2+</sup> concentration in the endoplasmic reticulum.	<i>FEBS Lett</i>	580	5635-5640	2006
Gao J., <b>Katagiri H.</b> , Ishigaki Y., Yamada T., Ogihara T., Imai J., Uno K., Hasegawa Y., Kanzaki M., Yamamoto TT., Ishibashi S., Oka Y	Involvement of apolipoprotein E in excess fat accumulation and insulin resistance.	<i>Diabetes</i>	56	24-33	2007

発表者氏名	論文タイトル名	発表誌名	巻号	ページ	出版年
Takahashi, R., Ishihara, H., Takahashi, K., Tamura, A., Yamaguchi, S., Yamada, T., <b>Katagiri, H.</b> , Oka, Y,	Efficient and controlled gene expression in mouse pancreatic islets by arterial delivery of tetracycline-inducible adenoviral vectors.	<i>J. Mol. Endocrinol</i>		<i>in press</i>	2007
Okimoto H, Ishigaki Y, Koiwa Y, Hinikio Y, Ogihara T, Suzuki S, <b>Katagiri H.</b> , Ohkubo T, Hasegawa H, Kanai H, Oka Y	A novel method for evaluating human carotid artery elasticity: possible detection of early stage atherosclerosis in subjects with type 2 diabetes.	<i>Atherosclerosis</i>		<i>in press</i>	2007
Hasegawa Y, Ogihara T, Yamada T, Ishigaki Y, Imai J, Uno K, Gao J, Kaneko K, Ishihara H, Sasano H, Nakauchi H, Oka Y, <b>Katagiri H</b>	Bone Marrow (BM) Transplantation Promotes Beta Cell Regeneration after Acute Injury through BM Cell Mobilization	<i>Endocrinology</i>		<i>in press</i>	2007
田村明、石原寿光、鈴木進、平井完史、高橋累、山口賢、岡芳知、佐藤文俊、菅野記豊、 <u>片桐秀樹</u>	肝硬変を伴う2型糖尿病患者に見られた著明な高インスリン血症と低血糖発作	日本内科学会雑誌	95	1371-4	2006
<u>片桐秀樹</u>	臓器間代謝情報ネットワークによる代謝調節機構の発見～肥満・糖尿病の治療法開発に向けて～	ヒューマンサイエンス	17	14-18	2006
山田哲也、 <u>片桐秀樹</u>	脂肪組織の神経調節	分子細胞治療	5 (4)	318-324	2006
山田哲也、石垣泰、岡芳知、 <u>片桐秀樹</u>	食欲調節における腹腔内脂肪からの神経シグナルの役割	細胞工学	25 (7)	774-775	2006
荻原健英、 <u>片桐秀樹</u> 、岡芳知	インスリン抵抗性発現にかかわるインスリン受容体および受容体基質の役割	日本臨床 増刊号「メタボリックシンドローム」	64 (9)	126-131	2006
山田哲也、石垣泰、宇野健司、岡芳知、 <u>片桐秀樹</u>	神経ネットワークを用いた臓器間相互作用調節機構	実験医学	24 (16)	2490-2493	2006
犬飼浩一、 <u>片桐秀樹</u>	レジスチン	<i>Adiposience</i>	11 (3)	277-281	2006
石垣泰、 <u>片桐秀樹</u>	病態基盤としての肥満	脈管学	46 (4)	423-428	2006
長谷川豊、荻原健英、 <u>片桐秀樹</u> 、岡芳知	糖尿病・耐糖能異常	<i>Medical Practice</i>	23 (9)	1507-1510	2006

発表者氏名	論文タイトル名	発表誌名	巻号	ページ	出版年
Magesh S., Suzuki T., Miyagi T., <u>Ishida H.</u> , Kiso M.	Homology modeling of human sialidase enzymes NEU1, NEU3 and NEU4 based on the crystal structure of NEU2: Hints for the design of selective NEU3 inhibitors	<i>Journal of Molecular Graphics and Modelling</i>	25	196-207	2006
Attrill, H., Takazawa H., Witt S., Kelm S., Isecke R., Brossmer R., Ando T., <u>Ishida H.</u> , Kiso M.	The structure of Siglec-7 in complex with sialosides: leads for rational structure-based inhibitor design	<i>Biochemical Journal</i>	397 (2)	271-278	2006
Takaku H., Sato J., Ishida H., Inazu T., <u>Ishida H.</u> , Kiso M.	A chemical synthesis of UDP-LacNAc and its regioisomer for finding 'oligosaccharide transferases'	<i>Glycoconjugate Journal</i>	23	565-573	2006
Ando, H., Shimizu, H. Katano, Y., Koike, Y. Koizumi, S., <u>Ishida H.</u> Kiso, M.	Studies on the $\alpha$ -(1 $\rightarrow$ 4)- and $\alpha$ -(1 $\rightarrow$ 8)-fucosylation of sialic acid for the total assembly of the glycan portions of complex HPG-series gangliosides	<i>Carbohydrate Research</i>	341	1522-1532	2006
Makimura Y., Watanabe S., Suzuki T., Suzuki Y., <u>Ishida H.</u> , Kiso M., Katayama T., Kumagai H., Yamamoto K.	Chemoenzymatic synthesis and application of a sialoglycopolymer with a chitosan backbone as a potent inhibitor of human influenza virus hemagglutination	<i>Carbohydrate Research</i>	341	1803-1808	2006
Fuse, T., Ando, H. Imamura, A., Sawada, N. <u>Ishida H.</u> , Kiso, M. Ando T.	Synthesis and enzymatic susceptibility of a series of novel GM2 analogs	<i>Glycoconjugate Journal</i>	23	329-343	2006
Sawada, T., Hashimoto, T. Nakao, H., Suzuki T. <u>Ishida H.</u> , Kiso, M.	Why does avian influenza A virus hemagglutinin bind to avian receptor stronger than to human receptor? Ab initio fragment molecular orbital studies	<i>Biochemical and Biophysical research communications</i>	351	40-43	2006
Sawada, T., Hashimoto, T. Nakao, H., Shigematsu, M. <u>Ishida H.</u> , Kiso, M.	Conformational study of $\alpha$ -N-acetyl-D-neuraminic acid by density functional theory	<i>Journal of Carbohydrate Chemistry</i>	25(5)	387-405	2006

発表者氏名	論文タイトル名	発表誌名	巻号	ページ	出版年
Kimura, A., Imamura, A., Ando, H., <u>Ishida, H.</u> , Kiso, M.	A novel synthetic route to $\alpha$ -galactosyl ceramides and iGb3 using DTBS-directed $\alpha$ -selective galactosylation	<i>SYNLETT</i>	15	2379-2382	2006
Imamura, A., Kimura, A., Ando, H., <u>Ishida, H.</u> , Kiso, M.	Extended applications of Di-tert-butylsilylene-Directed $\alpha$ -Preedominant galactosylation compatible with C2-Participating groups toward the assembly of various glycosides.	<i>Chemistry European Journal</i>	12	8862-8870	2006
Hashimoto, M., Furuyashiki, M., Kaseya, R., Fukuda, Y., Akimaru, M., Aoyama, K., <u>Okuno, T.</u> , Tamura, T., Kirikae, T., Kirikae, F., Eiraku, N., Morioka, H., Fujimoto, Y., Fukase, K., Takashige, K., Moriya, Y., Kusumoto, S., Suda Y	Evidence of immunostimulating lipoprotein existing in the natural lipoteichoic acid fraction.	<i>Infect Immun</i>		in press	2007
岡本紀夫、濱田文、西村雅史、栗本拓治、田上雄一、周允元、 <u>奥野寿臣</u> 、三村治	Birdshot chorioretinopathyの1例.	<i>眼科</i>	48	1853-1858	2006
上田美子、岡本紀夫、 <u>奥野寿臣</u> 、三村治	Multiple evanescent white dot syndromeの1例.	<i>眼科臨床医報</i>	101	7-8	2007
<u>Kato, K.</u>	Glycobiological approach to understanding neural plasticity	<i>Trends in Glycoscience and Glycotechnology</i>		In press	2007
Noriyuki Maeda, Souichiro Miyazawa, Kosuke Shimizu, Tomohiro Asai, Sei Yonezawa, Sadaya Kitazawa, Yukihiro Namba, Hideo Tsukada and <u>Naoto Oku</u>	Enhancement of anticancer activity in antineovascular therapy is based on the intratumoral distribution of the active targeting carrier for anticancer drugs.	<i>Biol. Pharm. Bull.</i>	29	1936-1940	2006
Pongpun Siripong, Jantana Yahuafai, Kosuke Shimizu, Kanae Ichikawa, Sei Yonezawa, Tomohiro Asai, Kwanjai Kanokmedakul, Somsak Ruchirawat and <u>Naoto Oku</u>	Antitumor activity of liposomal naphthoquinone esters isolated from thai medicinal plant: <i>Rhinacanthus nasutus</i> Kurz.	<i>Biol. Pharm. Bull.</i>	29	2279-2283	2006

発表者氏名	論文タイトル名	発表誌名	巻号	ページ	出版年
Pongpun Siripong, Jantana Yahuafai, Kosuke Shimizu, Kanae Ichikawa, Sei Yonezawa, Tomohiro Asai, Kwanjai Kanokmedakul, Somsak Ruchirawat and <u>Naoto Oku</u>	Induction of apoptosis in tumor cells by three naphthoquinone esters isolated from thai medicinal plant: <i>Rhinacanthus nasutus</i> Kurz.	<i>Biol. Pharm. Bull.</i>	29	2070-2076	2006
Pongpun Siripong, Kwanjai Kanokmedakul, Suratsawadee Piyaviriyagul, Jantana Yahuafai, Rittichai Chanpai, Somsak Ruchirawat and <u>Naoto Oku</u>	Antiproliferative naphthoquinone esters from <i>Rhinacanthus nasutus</i> Kurz. roots on various cancer cells.	<i>J. Trad. Med.</i>	23	166-172	2006
Yasuyuki Sadzuka, Koji Tokutomi, Fumiaki Iwasaki, Ikumi Sugiyama, Toru Hirano, Hiroyuki Konno, <u>Naoto Oku</u> and Takashi Sonobe	The phototoxicity of photofrin was enhanced by PEGylated liposome in vitro.	<i>Cancer Lett.</i>	241	42-48	2006
Noriyuki Akita, Fukuto Maruta, Leonard W. Seymour, David J. Kerr, Alan L. Parker, Tomohiro Asai, <u>Naoto Oku</u>	Identification of oligopeptides binding to peritoneal tumors of gastric cancer	<i>Cancer Sci.</i>	97	1075-1081	2006
清水広介、奥直人	第2章 遺伝子導入のためのDDS技術、方法論 5. リポソームによるターゲティング 「ウイルスを用いない遺伝子導入法の材料、技術、方法論の新たな展開」 (原島秀吉、田畑泰彦 編)	遺伝子医学 MOOK	5	130-134	2006
浅井知浩、奥直人	リポソーム応用の新展開 特集：がん領域におけるドラッグデリバリーシステム (DDS)	最新医学	61	1084-1091	2006
浦上武雄、奥直人	siRNA実用化の鍵をにぎるDDS	ファルマシア	42	1217-1222	2006
Arimura K, <u>Arima N</u> , Matsushita K, Akimoto M, Park C-Y, Uozumi K, and Tei C.	High incidence of morphological myelodysplasia and aototic bone marrow cells in Behcet's disease.	<i>Journal of Clinical Immunology</i>		PMID: 17235688	2007
Akimoto M, Kozako T, Sawada T, Matsushita K, Ozaki A, Hamada H, Kawada H, Yoshimitsu M, Tokunaga M, Haraguchi H, Uozumi K, <u>Arima N</u> , and Tei C.	Anti-HTLV-1 Tax Antibody and Tax-specific Cytotoxic T Lymphocyte are Associated with a Reduction in HTLV-1 Proviral Load in Asymptomatic Carriers	<i>Journal of Medical Virology</i>			In press

発表者氏名	論文タイトル名	発表誌名	巻号	ページ	出版年
Suzuki S., Uozumi K., Maeda M., Yamasuji Y., Hashimoto S., Komorizono Y., Owatari S., Tokunaga M., Haraguchi K. <u>Arima N.</u>	Adult T-cell leukemia in a liver transplant recipient that did not progress after onset of graft rejection.	<i>Int J Hematol</i>	83	429-432	2006
Kozako T, <u>Arima N.</u> , Toji S, Masamoto I,*Akimoto M, Hamada H, Che X-F,Fujiwara H, Matsushita K,Tokunaga M, Haraguchi K, Uozumi K, Suzuki S, Takezaki T, and Sonoda S	Reduced Frequency, Diversity, and Function of Human T-cell Leukemia Virus Type 1-specific CD8+ T-cell in Adult T-cell Leukemia Patients	<i>J Immunol</i>	177	5718-5726	2006
Che X-F, Zheng C-L, Mutoh M, Owatari S, Gotanda T, Jeung H-C, Furukawa T, Ikeda R, Haraguchi M, <u>Arima N.</u> , Tanaka Y, Akiyama S.	Overexpression of surviving I primary ATL cells and sodium arsenite induces apoptosis by down-regulating surviving expression in ATL cell lines.	<i>Blood</i>	2005	4880-4887	2006
Owatari S, Uozumi K, Tokunaga M, Tokumaga M, Haraguchi K, Suzuki S, <u>Arima N.</u>	Adult T-cell leukemia/lymphoma in a 21-year-old man.	<i>Clin. Lab. Haem.</i>	28	141-144	2006



研 究 成 果 の 刊 行 物 ・ 別 刷

**SUGAR-IMMOBILIZED GOLD NANO-PARTICLES (SGNP): NOVEL BIOPROBE FOR THE ON-SITE ANALYSIS OF THE OLIGOSACCHARIDE-PROTEIN INTERACTIONS**

Yasuo Suda<sup>1,2</sup>, Yuko Kishimoto<sup>2</sup>, Tomoaki Nishimura<sup>1,2</sup>, Saktiko Yamashita<sup>2</sup>, Mina Hamamatsu<sup>1</sup>, Akihiro Saito<sup>1</sup>, Masaki Sato<sup>1</sup>, and Masahiro Wakao<sup>1</sup>

<sup>1</sup>Department of Nanostructure and Advanced Materials, Kagoshima University, 1-21-40, Kohrimoto, Kagoshima, Japan

<sup>2</sup>Sugar Chip R&D, Japan Science and Technology Agency, Kobe, Japan

**Introduction**

Oligosaccharides are increasingly being recognized as important partners in receptor-ligand binding and cellular signaling<sup>1</sup>. Specific structural attributes of the oligosaccharide determine their biological functions, through distinct binding interactions with proteins, other oligosaccharides, or cells. We have developed a chip technology, in which structurally defined oligosaccharides are two-dimensionally immobilized on a surface, which mimics nature<sup>2</sup>. The combination of our technology with Surface Plasmon Resonance (SPR) is a very powerful tool for the real-time study of the specific interactions between biological molecules, and could be used as a high-throughput screening method or as a novel diagnosis technology, since the experiment can be done without any labeling of targets. However, SPR experiments need particular and expensive equipment, and so can hardly be performed on-site, such as a patient's bedside in the hospital. To establish an on-site analysis, we apply our immobilization method to gold nano-particles (GNP) to prepare sugar-immobilized gold nano-particles (SGNP), and report the visual detection of the sugar-protein interaction and the isolation of the specific sugar-binding protein in this manuscript.

**Experimental**

**Materials.** All reagents were used without further purification. Sodium tetrachloroaurate was purchased from Nacalai Tesque (Kyoto, Japan). Proteins were purchased as follows: Concanavalin A (Con A) from EY-Laboratories (CA, USA); RCA120 from HONEN (Tokyo, Japan); bovine Serum Albumin (BSA) from (MS, USA). Reagents for SDS-PAGE were obtained from Nacalai Tesque.

**Instrumentation.** UV-VIS spectra were measured using Nano-drop (Nano drop Tech., DW, USA). Mass spectrometry was performed by Voyager DE-Pro or Mariner<sup>TM</sup> (AppliedBiosystems, CA, USA). JEM-3010 (JEOL, Tokyo, Japan) was used as a transmittance electron microscope (TEM) for GNP and SGNP. NMR spectra of the compounds were obtained on a JEOL ECA-600 spectrometer.

**Synthesis of Glc $\alpha$ 4Glc-mono (Ligand-conjugate containing  $\alpha$ -D-glucoside).** Mono-valent linker compound (10.0 mg, 34  $\mu$ mol) was dissolved in 1.0 ml of dimethylacetamide (DMAc). To the solution, were added maltose (12.2 mg, 34  $\mu$ mol) dissolved in 0.8 ml of distilled water and 2 ml of acetic acid. The reaction solution was kept on stand at 37 °C for 24 h. To the solution, NaCNBH<sub>3</sub> (21.3 mg, 340  $\mu$ mol) dissolved in 2 ml of distilled water was added. Then, the reaction solution was further kept on stand at 37 °C. After 72 h, the reaction was quenched by adding 2 ml of acetone. After removing organic solvent by evaporation, the reaction mixture was lyophilized. The purification was done by ODS and GPC. The purified product was characterized by <sup>1</sup>H NMR and MS.

**Synthesis of Gal $\beta$ 4Glc-mono (Ligand-conjugate containing  $\beta$ -D-galactoside).** By a similar protocol described above, the objected compound was prepared. Lactose was used instead of maltose.

**Synthesis of Glc $\alpha$ 4Glc-GNP ( $\alpha$ -D-Glucoside immobilized SGNP).** To 1 mM of aqueous solution of NaAuCl<sub>4</sub>, NaBH<sub>4</sub> was added to 5 mM (final concentration) with stirring. Then Glc $\alpha$ 4Glc-mono, a ligand-conjugate, was added with stirring. Then, the reaction solution was dialyzed against distilled water and phosphate-buffered saline containing 0.05% tween-40 (PBS-T).

**Synthesis of Gal $\beta$ 4Glc-GNP ( $\beta$ -D-Galactose immobilized SGNP).** A similar protocol described above was applied to prepare Gal $\beta$ 4Glc-GNP. The ligand-conjugate, Gal $\beta$ 4Glc-mono, was used instead of Glc $\alpha$ 4Glc-mono.

**Binding experiment.** 50  $\mu$ L of SGNP colloid solution (OD at 520 nm = 0.3 /mm) was placed in 96 well plastic micro plate. To each well, proteins

dissolved in PBS-T (50  $\mu$ L) were added with changing the concentration. The plate was gently rotated at 50 rpm for 1 h.

**Isolation of protein.** 50  $\mu$ L of SGNP (OD at 520 nm = 0.3 /mm, PBS-T) was placed in 1.5 mL eppendorf tube. To the tube, protein solution was added. The tube was rotated at 50 rpm for 2 h to obtain the precipitate of SGNP. After removing the supernatant, the precipitate was washed with PBS-T and distilled water. Then, aqueous solution of monosaccharide (ex. D-glucose in the case of Glc $\alpha$ 4Glc-GNP; D-galactose in the case of Gal $\beta$ 4Glc-GNP) was added to the tube. After dissolving the precipitate into gold colloidal solution using vortex mixer for 10 seconds, 10  $\mu$ L of the colloidal solution was removed for the detection of the protein by SDS-PAGE.

**Results and Discussion**

**Preparation of ligand-conjugates.** The synthesis of Glc $\alpha$ 4Glc-mono was depicted in Figure 1. An optimized reductive amination reaction and well-designed linker compound<sup>3</sup>, in which aromatic amino group and the cyclic disulfide moiety were key units, were selected. The yield was about 50%, but major loss was occurred at the purification stage.

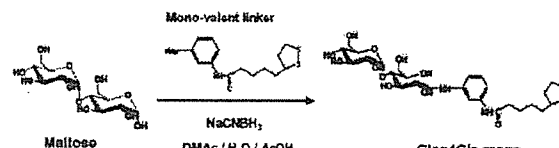


Figure 1. Preparation of ligand-conjugate (Glc $\alpha$ 4Glc-mono)

**Preparation of sugar-immobilized gold nano-particle (SGNP).** GNP was first prepared according to Brust *et al.*<sup>3</sup> using NaBH<sub>4</sub> as a reducing reagent. Without isolation of GNP, the ligand-conjugate was added into the preparing solution of GNP *in situ*. The concentration of the ligand-conjugate affected the preparation of SGNP. As shown in Figure 2, immature SGNP was aggregated during the dialysis. The best result was obtained when 100  $\mu$ M (final concentration) of ligand conjugate was used against 1 mM of sodium tetrachloroaurate for the starting GNP solution. The color of SGNP was purple, showing  $\lambda_{max}$  at 520 nm. The size of SGNP measured by TEM (Figure 3) were about 2 - 10 nm, which were smaller than GNP (10 - 40 nm) prepared by the conventional method using citric acid. From the size and the optimized concentration of ligand-conjugate, it was speculated that about 8 ligand-conjugates were immobilized on one molecule of GNP in average. The obtained SGNP is very stable and can be stored as lyophilized powder.

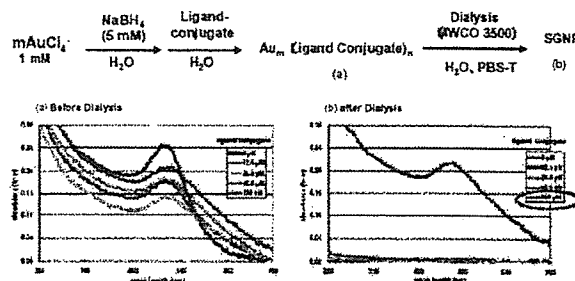


Figure 2. Protocol for the preparation of SGNP (upper) and changes of UV-VIS spectra during the preparation (lower).

**Binding experiment using SGNP.** Figure 4 shows the results of the interaction between protein and sugar moiety immobilized on the GNP. In the case of Con A, which is known to have a binding potency with  $\alpha$ -glucose or  $\alpha$ -mannose, the aggregates were formed in only Glc $\alpha$ 4Glc-GNP series, not in Gal $\beta$ 4Glc-GNP. In contrast, in the case of RCA 120, which is a  $\alpha$ - $\beta$ -galactose binding lectin protein, the aggregates were formed in Gal $\beta$ 4Glc-GNP, but not in Glc $\alpha$ 4Glc-GNP. In the case of BSA, which is not a lectin protein used as negative control, no aggregates were formed in both cases. It is important to note that those changes can be detected visually. These results indicate that

our SGNP may have good property for the binding interaction between oligosaccharides and proteins on-site. The optical density (OD) at 520 nm of supernatant (solution) was monitored and plotted against the concentration of protein in Figure 4. It was cleared that the specific binding between  $\alpha$ -Glc and Con A or  $\beta$ -Gal and RCA120 was detected. Also from this OD-values, the dissociation constant ( $K_D$ ) was calculated: 490 nM for ConA and 330 nM for RCA120. These values are similar to those obtained by SPR experiments.

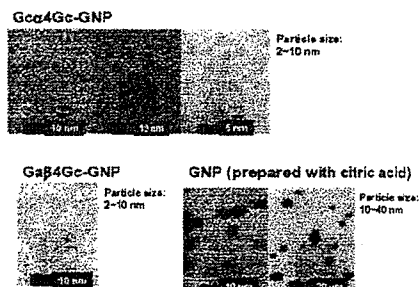


Figure 3. TEM images of SGNP (Glc $\alpha$ 4Glc-GNP: upper, Gal $\beta$ 4Glc-GNP: lower left) and GNP prepared by the conventional method using citric acid. Bars in the images represent scales.

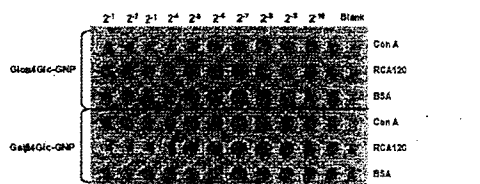


Figure 4. Results of the binding interaction between proteins and sugar moiety immobilized on SGNP. Protein solutions were diluted to 1/2 from the original concentrations.

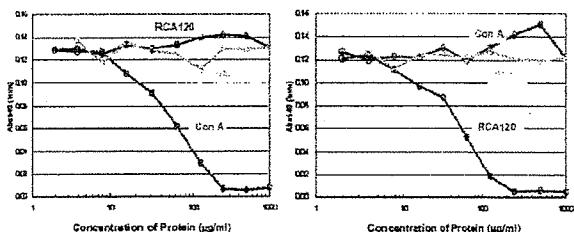


Figure 5. Results of the binding interaction between proteins and sugar moiety immobilized on SGNP monitored by OD at 540 nm. Left: Glc $\alpha$ 4Glc-GNP; Right: Gal $\beta$ 4Glc-GNP.

**Isolation and purification of proteins bound to SGNP.** SGNPs were applied for an easy and quick isolation of carbohydrate binding lectin protein as shown in Figure 6. SGNP was aggregated by the addition of the appropriate protein (Con A to Glc $\alpha$ 4Glc-GNP, RCA 120 to Gal $\beta$ 4Glc-GNP). After washing, when appropriate monosaccharide (D-glucose to Glc $\alpha$ 4Glc-GNP, D-galactose to Gal $\beta$ 4Glc-GNP) was added, the aggregate turned into a colloidal solution. The effect of the concentration is shown in Figure 7. It was found the OD at 530 nm was recovered, suggesting a re-formation of SGNP colloidal solution. The bound protein in the aggregates was eluted as shown in Figure 8 by the competitive binding of the monosaccharide to the protein bound to immobilized sugar moiety on GNP, suggesting quick isolation of the target protein. A similar protocol was applied for the easy purification of protein from the mixture. Figure 9 shows the results of SDS-

PAGE. From the mixture of Con A and BSA, Con A was purified by one step using Glc $\alpha$ 4Glc-GNP.

### Conclusions

It was obvious that sugar-immobilized gold nano-particle was very useful for the on-site detection of binding interaction between sugar-moiety and protein, and for the quick and easy isolation/purification of carbohydrate binding proteins. We have prepared so far more than 30 kinds of SGNP. More applications of SGNP, such as diagnosis method for specific diseases upon infection, are now on-going.

**Acknowledgements.** The authors of this paper would like to thank SHORAI Foundation for Science and Technology, SUZUKEN Memorial Foundation, Japan Science and Technology Agency (JST), and Japan Ministry of Health, Labor and Welfare for financial support of this research.

### References

- (1) Varki, A. in *Essentials of Glycobiology*, (Eds.: Varki, A., Cummings, R., Esko, J., Freeze, H., Hart, G., and Marth, J.), Cold Spring Harbor Laboratory Press. Cold Spring Harbor, New York, NY, 1999, 57, and references therein.
- (2) Suda, Y. et al. WO 2004/022583 A1; WO 2004/022565 A1.
- (3) Brust M., et al. *J. Chem. Soc. Chem. Commun.*, 1994, 801.

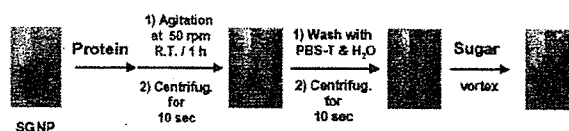


Figure 6. Protocol for the isolation/purification of protein(s) which bound immobilized sugar moiety specifically.

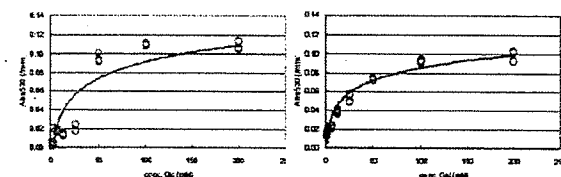


Figure 7. Recovery of the colloidal solution of SGNP by the addition of monosaccharide. Left: D-glucose for Glc $\alpha$ 4Glc-GNP, Right: D-galactose for Gal $\beta$ 4Glc-GNP.

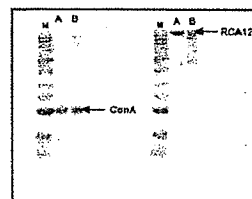


Figure 8. SDS-PAGE of colloidal solution of SGNP. Left: Con A was added to Glc $\alpha$ 4Glc-GNP, Right: RCA 120 was added to Gal $\beta$ 4Glc-GNP. M: marker protein, A: original protein solution, B: colloidal solution after the addition of monosaccharide.

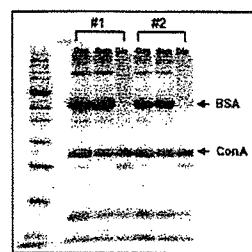


Figure 9. SDS-PAGE of colloidal solution of SGNP. #1: 500  $\mu$ g/ml of BSA and 300  $\mu$ g/ml of Con A was mixed in the original solution (Org). #2: 250  $\mu$ g/ml of BSA and 300  $\mu$ g/ml of Con A was mixed in the original solution (Org). Sep represents supernatant of the aggregate. Dis represents the recovered colloidal solution.

# Heparin-II Domain of Fibronectin Is a Vascular Endothelial Growth Factor–Binding Domain

## Enhancement of VEGF Biological Activity by a Singular Growth Factor/Matrix Protein Synergism

Errol S. Wijelath, Salman Rahman, Mayumi Namekata, Jacqueline Murray, Tomoaki Nishimura, Zohreh Mostafavi-Pour, Yatin Patel, Yasuo Suda, Martin J. Humphries, Michael Sobel

**Abstract**—We describe extracellular interactions between fibronectin (Fn) and vascular endothelial growth factor (VEGF) that influence integrin-growth factor receptor crosstalk and cellular responses. In previous work, we found that VEGF bound specifically to fibronectin (Fn) but not vitronectin or collagens. Herein we report that VEGF binds to the heparin-II domain of Fn and that the cell-binding and VEGF-binding domains of Fn, when physically linked, are necessary and sufficient to promote VEGF-induced endothelial cell proliferation, migration, and Erk activation. Using recombinant Fn domains, the C-terminal heparin-II domain of Fn (type III repeats 13 to 14) was identified as a key VEGF-binding site. Mutation of the heparin-binding residues on FnIII<sub>13-14</sub> abolished VEGF binding, and peptides corresponding to the heparin-binding sequences in FnIII<sub>13-14</sub> inhibited VEGF binding to Fn. Fn fragments containing both the  $\alpha_5\beta_1$  integrin-binding domain (III 9 to 10) and the VEGF-binding domain (III 13 to 14) significantly enhanced VEGF-induced EC migration and proliferation and induced strong phosphorylation of the VEGF receptor and Erk. Neither the cell-binding or VEGF-binding fragment of Fn alone had comparable VEGF-promoting effects. These results suggest that the mechanism of VEGF/Fn synergism is mediated extracellularly by the formation of a novel VEGF/Fn complex requiring both the cell-binding and VEGF-binding domains linked in a single molecular unit. These data also highlight a new function for the Fn C-terminal heparin-binding domain that may have important implications for angiogenesis and tumor growth. (*Circ Res.* 2006;99:853-860.)

**Key Words:** endothelial cell differentiation ■ endothelial cell growth ■ endothelial cells ■ fibronectin ■ integrins ■ signal transduction ■ vascular endothelial growth factor ■ vascular endothelial growth factor receptors

Fibronectin (Fn) and vascular endothelial growth factor (VEGF or VEGF-A) are key regulators of blood vessel growth.<sup>1-3</sup> Gene deletion studies have demonstrated that both Fn and VEGF, and their cognate receptors  $\alpha_5\beta_1$  and VEGF receptor-2 (VEGFR-2), are critical for vascular development.<sup>4-9</sup> During vascular growth, endothelial cells (ECs) are recruited into a tightly controlled program of cell activation, gene expression, adhesion, motility, and proliferation.<sup>10,11</sup> Crosstalk between integrins and growth factor receptors (receptor tyrosine kinases, RTKs) is a key part of this control process.<sup>12-16</sup> EC responses to growth factors like VEGF are modulated by the outside-in signals conveyed from integrins, reflecting the conditions of the extracellular milieu. Hence, the local mixture of extracellular matrix (ECM) proteins as well as the type and density of integrins expressed by the cell may modulate its responses to growth factors. Integrin

engagement by a specific matrix protein can transactivate VEGF receptors, as shown by Groopman and colleagues for fibronectin (Fn) and VEGF receptor-3, via  $\alpha_5\beta_1$ ,<sup>17</sup> and by Moro et al for epidermal growth factor receptor.<sup>18</sup> Others have shown that  $\beta_1$  activation by Fn can modulate VEGF responses,<sup>19</sup> and that  $\beta_3$  activation may increase VEGF production in tumor cells.<sup>20</sup> Conversely, occupancy of VEGFR-2 by VEGF can activate integrins. Byzova et al have shown that VEGF activates both  $\alpha_v\beta_3$  and  $\alpha_5\beta_1$  on ECs.<sup>21</sup> Finally, integrins and receptor tyrosine kinases (RTKs) share a number of important signaling molecules, including Src, FAK, and phosphatidylinositol 3-kinase (PI3K).<sup>13</sup> Our previous work has focused on the specificity of interactions between Fn and VEGF, and their cognate receptors,  $\alpha_5\beta_1$  and VEGFR-2.<sup>22,23</sup> We found VEGF bound to Fn and that platelets secreted VEGF/Fn complexes. In the presence of the

Original received April 26, 2006; revision received August 29, 2006; accepted September 14, 2006.

From the Department of Surgery (E.S.W., M.N., J.M., M.S.), Division of Vascular Surgery, Veterans Affairs Puget Sound Health Care System and the University of Washington School of Medicine, Seattle; The Thrombosis and Vascular Remodeling Laboratory (S.R., Y.P.), Kings College London School of Medicine at St. Thomas Hospital, London, UK; Department of Nanostructure and Advanced Materials (T.N., Y.S.), Graduate School of Science and Engineering and Venture Business Laboratory, Kagoshima University, Japan; and Wellcome Trust Center for Cell-Matrix Research (Z.M.-P., M.J.H.), School of Biological Sciences, University of Manchester, UK.

Correspondence to Errol S. Wijelath, PhD, Research Service-151, 1660 S Columbian Way, Seattle, WA 98108. E-mail errolw@u.washington.edu  
© 2006 American Heart Association, Inc.

*Circulation Research* is available at <http://circres.ahajournals.org>

DOI: 10.1161/01.RES.0000246849.17887.66

ligands VEGF and Fn, their corresponding receptors coimmunoprecipitated. Fn, but not vitronectin, induced sustained mitogen-activated protein kinase (MAPK) activation in response to VEGF. Thus we predicted that the VEGF-enhancing activities of Fn were attributable, in part, to its binding to VEGF.

This present study was undertaken to more precisely map the binding site(s) for VEGF within the C-terminal regions of Fn and to determine the mechanisms of Fn-induced enhancement of VEGF activity. Using recombinant Fn fragments, and synthetic peptides, we have mapped the VEGF-binding site to the established heparin-II (Hep-II) site of Fn type III modules 13 to 14.<sup>24,25</sup> This VEGF-binding domain of Fn was found to be necessary but, by itself, was not sufficient for the promotion of VEGF biological activity. Only bivalent Fn constructs encompassing both the  $\alpha_3\beta_1$  and VEGF-binding domains significantly promoted endothelial migration, proliferation, and sustained Erk phosphorylation. Purely costimulatory signaling (via occupancy of integrin and VEGFR-2 receptors) was a weaker influence on VEGF activity, because mixtures of VEGF with monovalent Fn fragments containing cell- and VEGF-binding domains showed less migration, proliferation, and no late phase of Erk phosphorylation.

## Materials and Methods

### Cell Culture

Human umbilical vein ECs (HUVECs) (Cascade Biologics) were maintained in MCDB-131 growth medium (MCDB-131 medium containing 5% FBS, 2 ng/mL basic fibroblast growth factor [bFGF], 10 ng/mL VEGF, and 10  $\mu$ g/mL heparin). HUVECs between passage 3 to 8 were used for experiments.

### cDNA Construction

Human Fn cDNA was obtained by RT-PCR using human liver mRNA and sequenced to verify no base changes during PCR amplification. The Fn type III modules were obtained by PCR amplification using Fn cDNA as template. We used the following nomenclature for describing the recombinant Fn constructs: rFnIII<sub>9-10</sub> indicates recombinant Fn protein encompassing type III repeats 9 to 10; rFnIII<sub>9-10/12-14</sub>, a single protein encompassing type III repeats 9 to 14, omitting 11. A rFnIII<sub>12-14</sub> with the heparin-binding sites on FnIII domains 13 and 14 mutated (Arg or Lys→Ser, termed "gag AC") was obtained as previously described.<sup>26</sup> For details on the construction of the rFn plasmids and their expression and purification, please see the online data supplement, available at <http://circres.ahajournals.org>.

### EC Migration Assay

EC chemotactic migration to VEGF (10 ng/mL; upper chamber) was studied in the presence of different rFn fragments (0.2  $\mu$ mol/L; bottom chamber). Ninety-six well ChemoTx microtiter plates (Neuro Probe Inc) were used, as previously described.<sup>22,27</sup> Positive and negative controls included native Fn, vitronectin, or albumin all at 10  $\mu$ g/mL, in the place of the tested rFn fragments.

### Endothelial Proliferation Assay

Early-passage HUVECs (3000 cells/well) in 96-well plates were cultured in MCDB-131 medium containing fibronectin-depleted FBS (0.25%). Cells were incubated with albumin, VEGF alone (10 ng/mL), or VEGF with native Fn (10  $\mu$ g/mL) or rFn fragments (0.2  $\mu$ mol/L) for 72 hours. Heparin was used at a final concentration of 1  $\mu$ g/mL. Cell growth was determined by using CyQuant reagent (Molecular Probes) according to the instructions of the manufacturer.

### Western Blot Analyses

For analysis of Erk phosphorylation,  $5 \times 10^5$  HUVECs were plated onto 60-cm<sup>2</sup> culture dishes and incubated overnight in MCDB-131 growth medium. Cells were then washed twice and incubated for 4 hours in serum-free MCDB-131 medium. Cells were stimulated with VEGF (10 ng/mL) or VEGF with different Fn combinations. At different time points, cells were lysed and Erk phosphorylation detected as previously described.<sup>28</sup> Signal densities were quantified by the NIH Image program, and the activation of phosphorylated protein was expressed as the fold increase over basal (unstimulated) levels, adjusted for total protein loading, measured from separate blots.

To measure VEGFR-2 phosphorylation, HUVECs ( $2 \times 10^6$  cells) were cultured for 48 hours in MCDB-131 growth medium. Before assay, cultures were washed and replaced with serum-free MCDB-131 containing ITS supplement (BD Bioscience) and incubated for a further 4 hours. Culture plates were then stimulated with a low dose of VEGF (1 ng/mL) in the absence or presence of rFnIII<sub>9-10/12-14</sub> for 2 minutes at 37°C. Cell lysates were incubated with anti-VEGFR-2 rabbit monoclonal antibodies (Cell Signaling) for 16 hours at 4°C and immune complexes precipitated with protein G sepharose. Protein samples were reduced, separated by Bis-Tris PAGE gels, transferred to polyvinylidene difluoride (PVDF) membranes, probed with anti-phospho VEGFR-2 antibodies and signals developed by chemiluminescence. Blots were stripped and reprobed with anti-VEGFR-2.

### <sup>125</sup>I-VEGF Solid-Phase Binding Assays

The measurement of direct binding of <sup>125</sup>I-VEGF to Fn fragments was performed as described previously.<sup>22</sup> For peptide competition assays, the same binding assay methods were used, with recombinant C-terminal rFn III<sub>9-10/12-14</sub> or rFnIII<sub>12-14</sub> immobilized on the plates.

### Surface Plasmon Resonance Analysis

Surface plasmon resonance analysis (SPR) binding experiments were conducted to measure the equilibrium binding parameters between VEGF<sub>165</sub> and native fibronectin or rFnIII<sub>9-10/12-14</sub>. The detailed methods are described elsewhere.<sup>29</sup> In brief, a 2-channel SPR670M apparatus (Moritex Corp) was used with a running buffer of PBS, 0.05% Tween-20 at a flow rate of 15  $\mu$ L/min at room temperature. The matrix proteins were immobilized on the gold chip using *N*-hydroxysuccinimidyl coupling, sensograms recorded over a range of VEGF concentrations (25 to 800 nmol/L), and the kinetic binding parameters derived using the software of the manufacturer.

### Statistical Analysis

Individual experiments were performed at least in triplicate, and the data presented are the means and SEM of at least 3 to 4 independent experiments, as noted. The Student's *t* test was used to compare different treatments.

## Results

### Expression and Purification of Fibronectin Fragments

Figure 1 illustrates a schematic of the native fibronectin protein and the design of the recombinant fragments. Each protein was expressed and purified to homogeneity, as described in Materials and Methods. A Bis-Tris PAGE gel shows representative samples of the purified proteins.

### VEGF Binding to Recombinant Fn Domains and Competition by Peptides

We first measured the concentration dependence of <sup>125</sup>I-VEGF<sub>165</sub> binding to different immobilized recombinant Fn fragments. These experiments were all conducted in the absence of exogenous heparin, indicating that heparin is not a

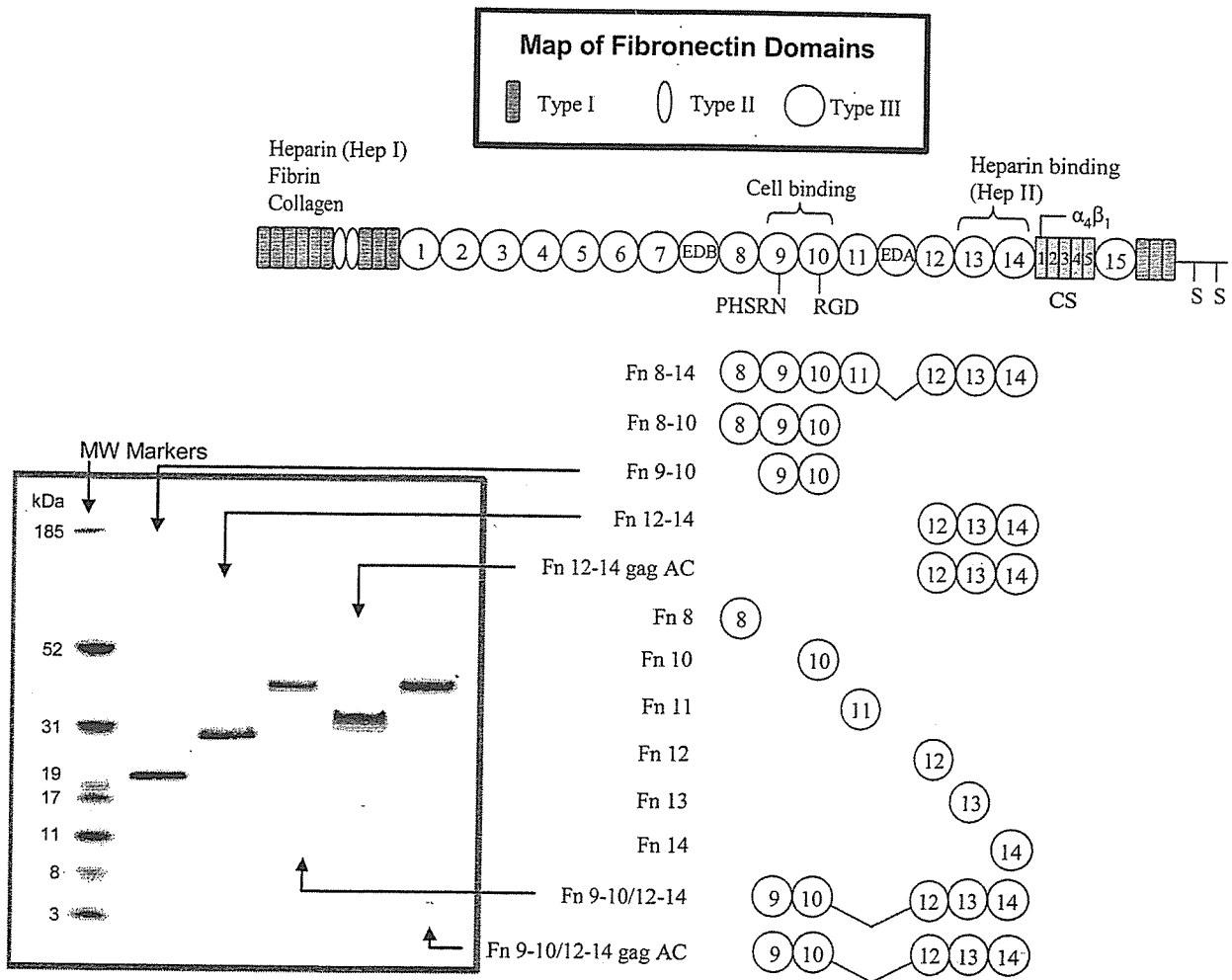


**Figure 1.** Schematic diagram of the domain structure of human Fn showing type I, type II, type III and their functions. Also diagrammed are the recombinant Fn type III domains used in this study, and on the left is a representative SDS-PAGE gel of purified fragments.

required cofactor for VEGF/Fn binding. In preliminary experiments, the actual quantity of experimental proteins deposited on the plate was measured by protein assay, confirming that the final density of coating was comparable for all test proteins. As shown in Figure 2, VEGF bound rFnIII<sub>12-14</sub> and rFnIII<sub>8-14</sub> in a concentration-dependent manner. Binding to rFnIII<sub>8-11</sub> was negligible. In subsequent binding assays, a coating concentration of 0.2 μmol/L was used for all proteins. The binding of VEGF to individual rFnIII domains was then evaluated. Figure 3A shows that VEGF does not bind significantly to any of the individual type III domains studied but did bind to all fragments containing FnIII<sub>13-14</sub> in continuity (ie, native Fn, rFn<sub>8-14</sub>, rFn<sub>12-14</sub>). Figure 3A and 3B shows that the linkage of the α<sub>5</sub>β<sub>1</sub> integrin-binding domain with rFnIII<sub>12-14</sub> (as in the constructs rFnIII<sub>8-14</sub> or III<sub>9-10/12-14</sub>) further enhanced VEGF binding when compared with rFnIII<sub>12-14</sub> alone. The binding of VEGF to rFnIII<sub>8-14</sub> and rFnIII<sub>9-10/12-14</sub> when compared with native Fn was consistently higher, suggesting a higher affinity for these fragments. Surface plasmon resonance binding analysis was used to compare the VEGF affinities of rFnIII<sub>9-10/12-14</sub> to native Fn. The rFnIII<sub>9-10/12-14</sub> fragment had a 43% lower dissociation constant ( $K_d$ , 73.5 versus 129.3 nmol/L), a faster on-rate and a smaller

off-rate (supplemental Table I). Because the region of FnIII<sub>12-14</sub> is known to be an important heparin-binding region,<sup>24,25,30</sup> we wanted to determine whether the key heparin-binding residues of FnIII<sub>12-14</sub> were required for binding

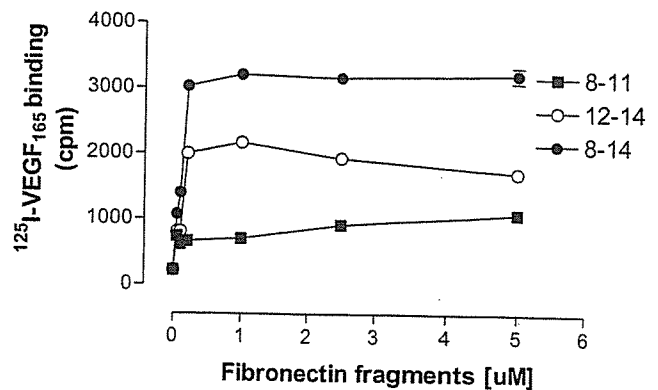


**Figure 2.** Concentration dependent <sup>125</sup>I-VEGF binding to immobilized rFn fragments. <sup>125</sup>I-VEGF was incubated for 2 hours on wells coated with increasing concentrations of rFn fragments. After washing, bound VEGF was eluted with 0.1 mol/L NaOH/1% SDS and radioactivity quantified in a gamma counter. Data are presented as the mean of triplicate determinations ± SEM.

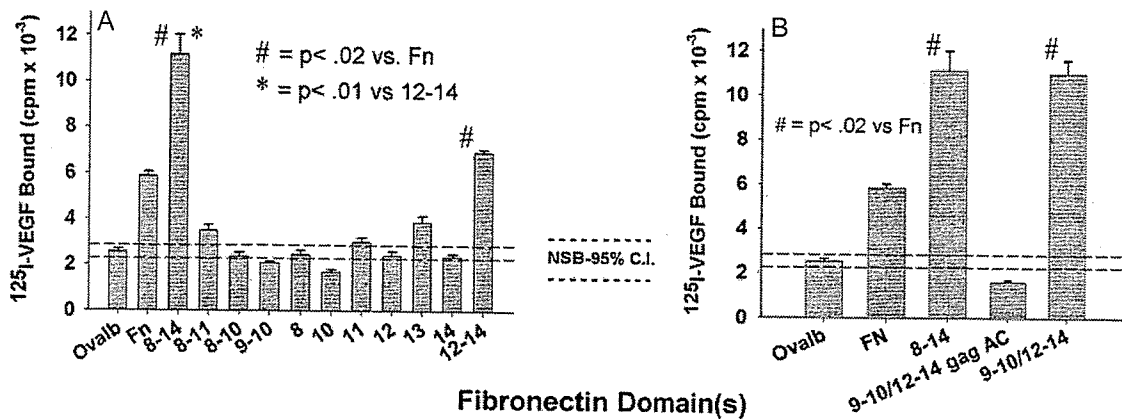


**Figure 3.** Mapping the VEGF-binding site on C-terminal Fn. A and B, <sup>125</sup>I-VEGF was incubated for 2 hours on wells coated with either individual or continuous rFn type III domains (0.2  $\mu$ mol/L) (A) or wells coated with rFn molecules encompassing both the integrin (9 to 10) and heparin-binding domains (12 to 14) (B). GagAC denotes mutation of the heparin-binding domains on type III module 13 and 14. After washing, bound VEGF was eluted with 0.1 mol/L NaOH/1% SDS and radioactivity quantified in a gamma counter. Data are the means  $\pm$  SEM of 3 to 4 independent experiments performed in triplicate. Dotted lines are 95% confidence intervals for control binding to albumin.

VEGF. To that end, the construct rFnIII<sub>9-10/12-14gagAC</sub> was prepared, in which the lysines and arginines of repeats 13 and 14 were mutated to serine, as previously described.<sup>26</sup> Figure 3B shows that the loss of these heparin-binding residues completely abolished VEGF binding.

Peptides (listed in the Table) encompassing the native heparin-binding regions in FnIII<sub>13-14</sub> were also used as soluble competitors of <sup>125</sup>I-VEGF binding to immobilized rFnIII<sub>12-14</sub> or rFnIII<sub>9-10/12-14</sub>. Two other peptides were also studied: a truncated version containing the putative key heparin-binding site of FnIII<sub>13</sub>, as well as a well-characterized heparin-binding site from the A1 domain of von Willebrand factor (vWf)<sup>31</sup> (Table). The results of peptide competition against VEGF binding to either rFnIII<sub>12-14</sub>, or rFnIII<sub>9-10/12-14</sub> substrates were not significantly different, so the data were pooled. The Table shows their estimated IC<sub>50</sub> (concentration that inhibits VEGF binding by 50%), and Figure 4 shows their inhibition curves. The most potent peptide was a heparin-binding region in FnIII<sub>14</sub> (core motif is PRAR). Second and third in rank order were the heparin-binding peptides derived from FnIII<sub>13</sub> (core motif PRRAR) and FnIII<sub>14</sub> (IYVIALKNNQKSEPLI-GRKKT), respectively. Truncating the heparin-binding domain of FnIII<sub>13</sub> eliminated its ability to compete with the immobilized Fn fragment for binding VEGF. Figure 4B correlates the potency of each peptide competitor with its total number of basic residues. The peptide charge accounts for some, but not all, of the apparent affinity of the peptides for VEGF. The most potent Fn peptide bears the same net

charge as the vWf heparin-binding peptide but has an IC<sub>50</sub> that is 600 times lower. The other 2 Fn peptides that share the PRRAR or PRAR motif possess the same number of heparin-binding residues but differ in affinity by 3.5-fold.

#### Specificity of Fn Domains That Promote VEGF-Mediated EC Cell Migration and Proliferation

We hypothesized that the formation of a unique extracellular VEGF/Fn complex promotes VEGF biological activity, mediated in part by the bivalent capacity of Fn to simultaneously bind  $\alpha_5\beta_1$  and VEGF. Accordingly, we measured the migration and proliferation of HUVECs in response to VEGF, in the presence of different native and recombinant matrix proteins. Figure 5A shows that there was minimal cellular migration toward VEGF in the absence of a matrix component, or with the addition of rFnIII<sub>12-14</sub> alone. Most of the proteins containing an integrin-binding domain (eg, vitronectin, rFn<sub>9-10</sub>, and rFn<sub>9-10/12-14gagAC</sub>) supported some migration to VEGF. In contrast, all bivalent matrices encompassing both the  $\alpha_5\beta_1$  and the VEGF-binding domains (FnIII<sub>8-14</sub> and FnIII<sub>9-10/12-14</sub>) increased cell migration by 2- to 3-fold. To distinguish between simple costimulatory signaling through the independent ligands (ie, integrin and growth factor receptor), chemotactic migration to VEGF was also measured in the presence of equivalent concentrations of a mixture of the isolated domains of rFnIII<sub>9-10</sub> and rFnIII<sub>12-14</sub>. This mixture did support a modicum of cell migration above baseline but did not increase migration to the extent induced by a bivalent Fn construct that linked both those domains.

We next examined whether rFn fragments promoted VEGF-induced HUVEC proliferation. As shown in Figure 5B, the extent of HUVEC proliferation in response to VEGF was enhanced in the presence of native Fn or rFnIII<sub>9-10/12-14</sub>, compared with the cell or VEGF-binding domains alone (rFnIII<sub>9-10</sub> or rFnIII<sub>12-14</sub>). Addition of heparin (1  $\mu$ g/mL) to the VEGF/Fn complex further augmented proliferation to the same extent heparin augmented proliferation of VEGF alone. A mixture of cell-binding and VEGF-binding fragments of Fn

#### Relative Inhibition of <sup>125</sup>I-VEGF<sub>165</sub> Binding by Heparin Binding Peptides

Protein	Peptide Sequence	IC <sub>50</sub> ( $\mu$ mol/L)
rFnIII <sub>13</sub>	1814 vspprrarvtdatettitisiwrkttetitgq	43
rFnIII <sub>13</sub> (truncated)	1814 ppprrarv	>1000
rFnIII <sub>14</sub>	1926 praritgyiikyekpgspprevvprprpgv	0.4
rFnIII <sub>14</sub>	1971 iyvialknnqksepligrkkt	150
von Willebrand factor	568 kdrrksrlrriassqvk	250

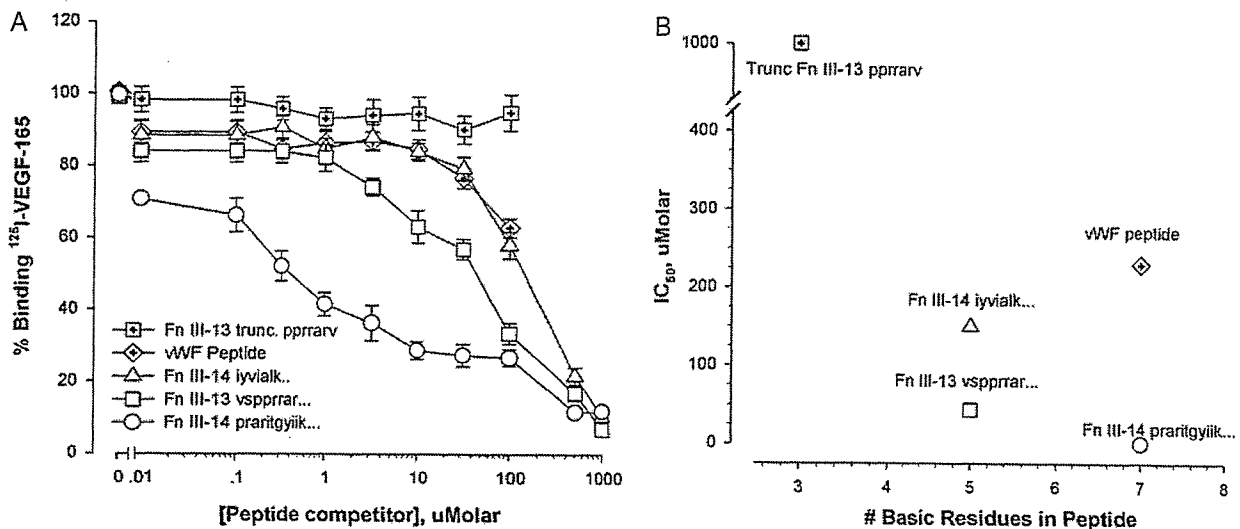


**Figure 4.** Peptide inhibition of VEGF binding to rFnIII<sub>9-10/12-14</sub>. <sup>125</sup>I-VEGF/Fn binding assays were performed in the presence of the peptides listed in the Table. A, Results are expressed as the percentage of VEGF binding observed in the absence of competitor (100%) and are the means  $\pm$  SEM of 4 to 6 independent experiments performed in triplicate. B, IC<sub>50</sub> ( $\mu$ M/L) was interpolated for each peptide and plotted against the total number of basic residues/peptide.

(at the same concentrations, 10  $\mu$ g/mL) showed less increase in proliferation compared with the divalent fragment.

### Modulation of VEGF-Mediated Signaling by Specific rFn Domains

Previously, our laboratory reported that VEGF/Fn complexes prolonged cell signaling induced by VEGF alone,<sup>22</sup> suggesting that such extracellular complexes may influence the magnitude and duration of cell signaling. Therefore, we examined the time course and sensitivity of Erk signaling to VEGF and different Fn domains. As shown in Figure 6, VEGF combined with native Fn produced a higher early (5 minutes) peak in phosphorylation, as well as more sustained activation at 1.5 to 3 hours. In comparison with native Fn, the rFnIII<sub>9-10/12-14</sub> induced an even higher early peak and a second peak of Erk activation at approximately 1.5 hour. A mixture of rFnIII<sub>9-10</sub> and rFnIII<sub>12-14</sub> (at the same individual concentrations as other fragments tested) did not induce any late Erk activation. When tested individually, the cell binding (rFnIII<sub>9-10</sub>) or VEGF-binding domains (rFnIII<sub>12-14</sub>) did not induce any late Erk activation. The divalent recombinant Fn fragment rFnIII<sub>9-10/12-14</sub>, significantly enhanced VEGF-induced Erk phosphorylation even at very low VEGF concentrations, between 0.1 to 0.5 ng/mL (Figure 7A and 7B). We next examined the influence of rFnIII<sub>9-10/12-14</sub> on the phosphorylation status of VEGFR-2 activated by a low dose of VEGF. Figure 7C shows that VEGF alone (1 ng/mL) did not significantly induce VEGFR-2 phosphorylation. However, in the presence of rFnIII<sub>9-10/12-14</sub>, significant VEGFR-2 phosphorylation was observed. Stimulation of cells with VEGF and either rFnIII<sub>9-10</sub> or rFnIII<sub>12-14</sub> did not show enhanced VEGFR-2 phosphorylation.

### Discussion

Based on our previous studies, we hypothesized that Fn may be a unique biological partner with VEGF: when Fn complexes with VEGF, their coordinated binding to their cognate

receptors enhance the specific cellular responses to VEGF. These extracellular events might be an important step in modulating the complex signaling pathways that lead from receptor ligation to cellular response. In this report we have physically mapped a key Fn-binding site for VEGF to the fibronectin C-terminal domain within type III repeats 13 to 14 (the Hep-II domain). Previous studies have established this site as a heparin-binding domain.<sup>24,25,30</sup> The Hep-II site is a major syndecan-binding site that plays a role in focal adhesion and stress fiber formation.<sup>32</sup> This report reveals a novel function for the Hep-II region as a site for VEGF binding, as well as a modulator of VEGF activity. Narrowing the binding site further, we observed that a peptide obtained from the N-terminal part of FnIII<sub>14</sub> was most effective at blocking VEGF binding, although other peptides representing heparin-binding sites were also inhibitory. Also, the heparin-binding properties of this Fn domain accounted for a significant portion of VEGF affinity. A heparin-mutant fragment did not bind VEGF, nor did it promote the biological activities of VEGF.

The second important finding from these experiments concerns the mechanism(s) of biological synergism between VEGF and Fn. We found that the VEGF-binding domain of Fn alone was not sufficient to enhance VEGF-mediated cell migration, proliferation, or growth factor signaling, even though it avidly bound VEGF. However, constructs of rFn in which the cell binding and VEGF-binding domains were physically linked dramatically enhanced these cellular responses, even more so than native Fn. rFn fragments containing only the cell-binding domain (FnIII<sub>9-10</sub>) did modestly enhance VEGF biological responses. These results may reflect the isolated contribution of the costimulatory signaling pathways that are known to exist between  $\alpha_5\beta_1$  and VEGFR-2 downstream to Erk. However, the current data suggest that these cooperative pathways are capable of a much more robust response when their receptors are occupied by a specialized VEGF/Fn complex. The rFnIII<sub>9-10/12-14</sub> construct



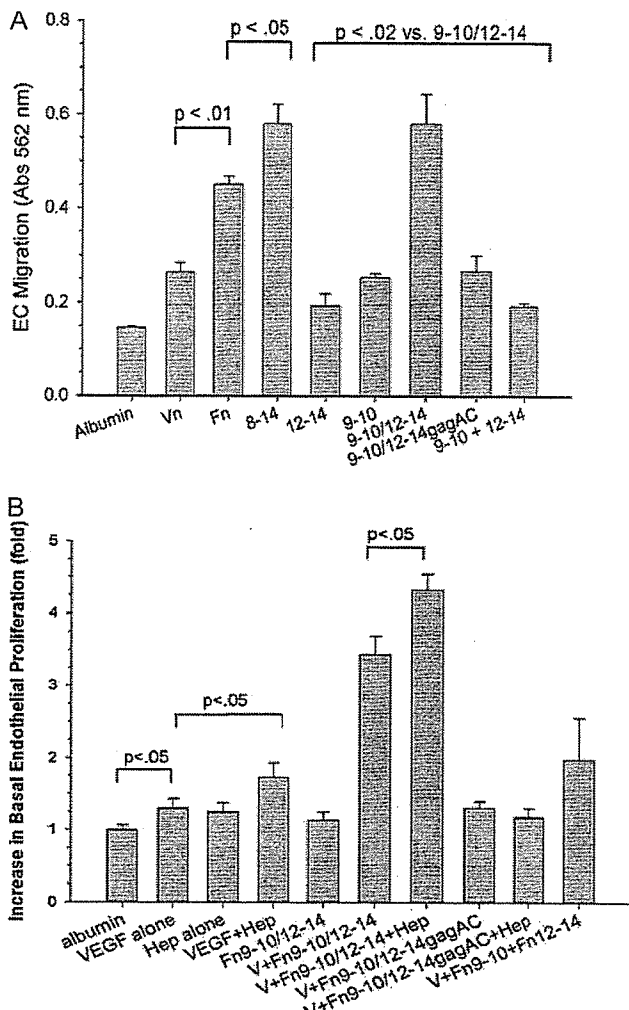


**Figure 5.** A, EC migration to VEGF in the presence of rFn fragments. HUVECs suspended in serum-free MCDB-131 medium containing 0.1% ovalbumin were seeded on to ChemoTx micro-titer plates and migration assay performed as described in Materials and Methods. Experiments were performed in triplicate and results expressed as mean±SEM. The final bar (indicated by 9-10 + 12-14) signifies treatment with a mixture of separate fragments of rFnIII<sub>9-10</sub> and rFnIII<sub>12-14</sub>, each at 0.2 μmol/L. B, EC proliferation in response to VEGF and rFn fragments. HUVECs (3000 cells/well) in 96-well plates were incubated in MCDB131 medium containing Fn-depleted FBS (0.25%). Cells were incubated with VEGF alone (10 ng/mL), VEGF (V) with native Fn (5 ng/mL), or rFn fragments (0.2 μmol/L). In some experiments, heparin (hep) was added at a final concentration of 1 μg/mL. Cell growth was determined after 72 hours. Experiments were done in triplicate and results are expressed as mean±SEM.

dramatically increased early Erk phosphorylation in response to VEGF, as well as inducing a major late peak in Erk activation at 1.5 hour. Thus, the coordinated extracellular modulation of these ligand/receptor interactions imposes more stringent directions on the intracellular signaling responses to VEGF.

Several lines of evidence suggest that the binding interaction between VEGF and the Hep-II domain are complex. VEGF did not bind to any single isolated immobilized type III repeat, yet VEGF bound to the Fn moieties containing the type III<sub>12-14</sub> repeats in continuity. This suggests that a more

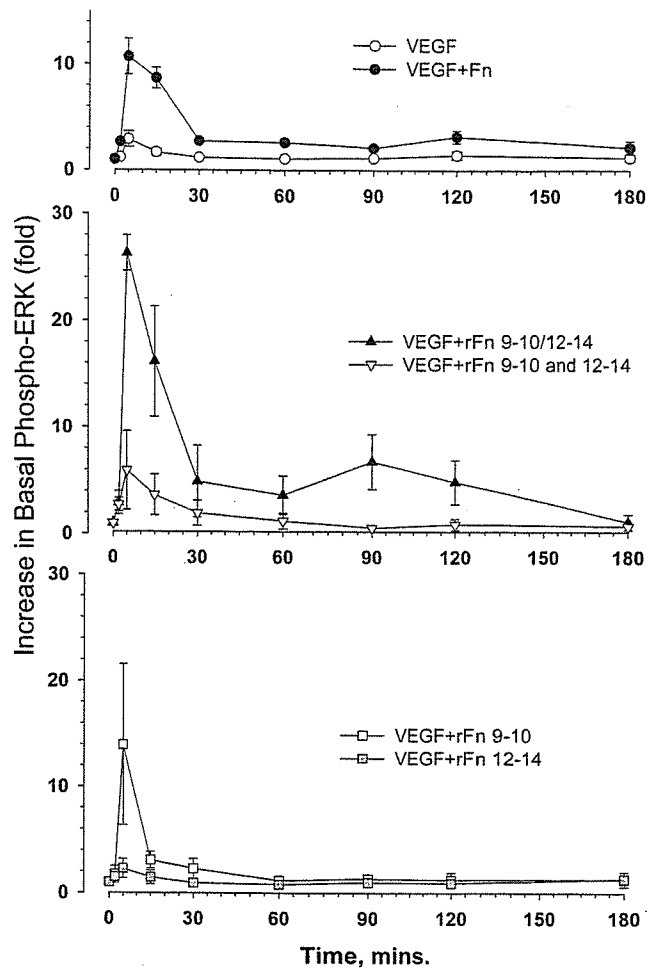


**Figure 6.** HUVEC Erk phosphorylation in response to VEGF and Fn moieties. HUVECs were exposed to 10 ng/mL of VEGF<sub>165</sub>, combined with the indicated Fn proteins (0.2 μmol/L). At the time points, cells were harvested and processed to measure phospho-Erk and total Erk protein by Western blotting. Each point on the graph is the mean of data obtained from 4 to 5 separate experiments and quantified as described in Materials and Methods.

complex tertiary structure within the Hep-II domain is necessary for VEGF binding. We observed that the constructs rFnIII<sub>8-14</sub> and rFnIII<sub>9-10/12-14</sub> bound more VEGF than rFnIII<sub>12-14</sub> alone. If FnIII<sub>9-10</sub> itself has no intrinsic VEGF-binding properties (as we observed), why should the larger construct that includes FIII<sub>9-10</sub> bind VEGF more avidly? These larger constructs (FnIII<sub>8-14</sub> and FnIII<sub>9-10/12-14</sub>) likely assume a conformation that more optimally displays the VEGF-binding sites. This is supported by the surface plasmon resonance studies, which showed that rFnIII<sub>9-10/12-14</sub> has a higher affinity for VEGF than native Fn. The bivalent Fn constructs encompassing both the integrin and VEGF-binding sites were also more biologically effective than native Fn. This again may be attributable to conformational differences, or their lack of large portions of the N and C-terminal regions of native Fn, which may play a negative modulatory role on VEGF function.

The heparin-binding properties of the FnIII<sub>12-14</sub> domain are clearly important, as illustrated by the failure of the heparin

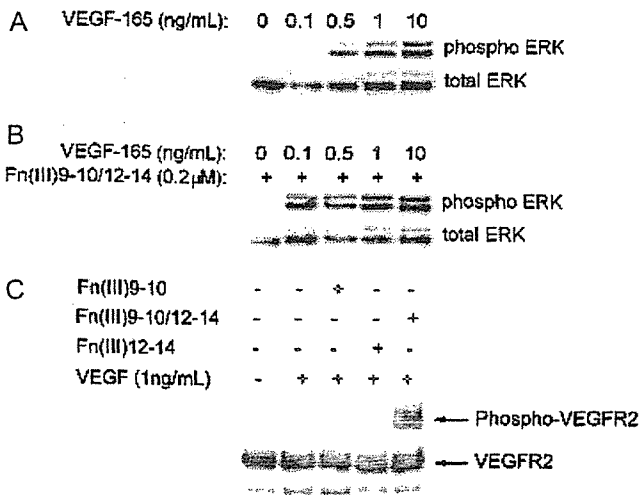


**Figure 7.** rFnIII<sub>9-10/12-14</sub> promotes Erk and VEGFR-2 phosphorylation at low VEGF concentration. A and B, HUVECs were exposed to varying concentrations of VEGF in the absence (A) or presence (B) of rFnIII<sub>9-10/12-14</sub> (0.2 μmol/L). Erk phosphorylation was determined by Western blotting. A representative blot from 2 separate experiments is shown. C, HUVEC cultures were stimulated with a low dose of VEGF (1 ng/mL) in the absence or presence of recombinant Fn fragments (0.2 μmol/L). Cell lysates were immunoprecipitated with anti-VEGFR-2 rabbit monoclonal antibodies followed by Western blotting with anti-phosphoVEGFR-2 rabbit monoclonal antibodies. Blots were stripped and reprobed with anti-VEGFR-2 antibodies. Experiments were repeated twice with similar results.

mutant fragment to bind or modulate VEGF activity. An alternative explanation for the behavior of the heparin mutant protein might be that the mutations altered the conformation of the Fn fragment. Weighing against that possibility are the studies of Mostafavi-Pour, which suggest that these mutations do not seriously alter the conformation of the protein.<sup>26</sup> Also, conformational changes of the mutant (or wild-type recombinant) protein would not explain why peptides selected from these heparin-binding domains successfully competed with rFnIII<sub>9-10/12-14</sub> for binding VEGF.

However, the peptide competition experiments also suggest that heparin-binding is not the entire VEGF/Fn binding story. The heparin-binding site in III<sub>13</sub> is thought to be the dominant interactive site for heparins,<sup>24,25</sup> yet its peptide domain was not the most potent at blocking VEGF binding, nor did its truncated form (the core heparin-binding residues) retain activity. Likewise, comparisons of peptide charge versus inhibitory potency suggest that nonelectrostatic, protein/protein interactions also account for VEGF/Fn binding. The vWf heparin-binding peptide, a highly charged, classical heparin-binding domain, had relatively low affinity for VEGF. This same vWf protein domain has been shown to interfere with cell adhesive strength and chemokinesis, presumably because of its interference with cell syndecan binding to the Hep-II domain of Fn.<sup>33</sup> Thus, this vWf heparin-binding domain may mimic the Fn Hep-II region, from the viewpoint of cell surface syndecans, but not from the perspective of VEGF. Finally, exogenous heparin was not required for rFn-VEGF binding (Figures 2 and 3). Heparin had the same mild stimulatory effect on the biological activity

of rFn/VEGF complexes as its effect on VEGF alone (which is well described).

A number of mechanisms have been suggested for integrin/growth factor synergism, many emphasizing pathways for intracellular signaling crosstalk. Signaling from  $\alpha_5\beta_1$  ligation (and syndecan engagement) can support or reinforce the downstream signaling from VEGFR-2 to Erk.<sup>22</sup> Conversely, VEGFR-2 activation can lead to integrin activation.<sup>21</sup> There exists some controversy as to whether the primary integrin synergizing with VEGF pathways is  $\alpha_5\beta_1$  or  $\alpha_v\beta_3$ .<sup>21,34</sup> This may be attributable to the type of ECM protein the cells are exposed to when stimulated with VEGF. Our previous studies suggest that VEGF/Fn complexes primarily cause a physical association between VEGFR-2 and  $\alpha_5\beta_1$ , but not  $\alpha_v\beta_3$ .<sup>22</sup> Moreover, we have also shown that VEGF/Fn complexes, as well as hepatocyte growth factor/Fn complexes, exist and are released from thrombin stimulated degranulating platelets.<sup>22,35</sup> These observations suggest that platelets may play a role in promoting angiogenesis. Recent studies by Kisucka et al have characterized the role platelets play in modulating angiogenesis in vivo.<sup>36</sup> We also observed that blockade of  $\alpha_5\beta_1$  profoundly inhibits VEGF-mediated migration and differentiation of endothelial progenitor cells.<sup>22,23</sup> These findings support the view espoused by Hynes and colleagues that  $\alpha_5\beta_1$  is a pivotal integrin for vascular development.<sup>6,37,38</sup> The current experiments suggest that the mechanism of Fn-induced enhancement of VEGF activity arises from both the formation of an extracellular complex interacting with the cell surface receptors and the resulting promotion of costimulatory signaling from integrin and VEGF receptor. Simple engagement of integrin and growth factor receptors by free, independent ligands does not induce the same quality or quantity of signaling, especially the late sustained Erk phosphorylation. In support of our hypothesis, recent studies of a parallel system demonstrated that binding of basic fibroblast growth factor to fibrinogen is required for the enhancement of basic fibroblast growth factor induced angiogenesis.<sup>39</sup>

More work will be needed to identify the interactive sites within VEGF and to define the role of the CS-1 domain of Fn also remains to be elucidated in this context. Further understanding of the structure/function relationship of these synergisms should permit the development and optimization of Fn-derived constructs that specifically amplify (or inhibit) the biological actions of VEGF.

### Sources of Funding

This research was supported by grants from the NIH (R01HL39903 and HL079182 to M.S.), the Department of Veterans Affairs Medical Research Service (to M.S.), the American Heart Association (to E.S.W.), and the Japan Science and Technology Agency (to Y.S.).

### Disclosures

None.

### References

1. Dvorak HF. Angiogenesis: update 2005. *J Thromb Haemost.* 2005;3:1835-1842.
2. Ferrara N, Gerber HP, LeCouter J. The biology of VEGF and its receptors. *Nat Med.* 2003;9:669-676.
3. Hynes RO, Bader BL, Hodivala-Dilke K. Integrins in vascular development. *Braz J Med Biol Res.* 1999;32:501-510.

4. Carmeliet P, Ferreira V, Breier G, Pollefeyt S, Kieckens L, Gertsenstein M, Fahrig M, Vandenhoek A, Harpal K, Eberhardt C, Declercq C, Pawling J, Moons L, Collen D, Risau W, Nagy A. Abnormal blood vessel development and lethality in embryos lacking a single VEGF allele. *Nature*. 1996;380:435-439.
5. Ferrara N, Carver-Moore K, Chen H, Dowd M, Lu L, O'Shea KS, Powell-Braxton L, Hillan KJ, Moore MW. Heterozygous embryonic lethality induced by targeted inactivation of the VEGF gene. *Nature*. 1996;380:439-442.
6. Francis SE, Goh KL, Hodivala-Dilke K, Bader BL, Stark M, Davidson D, Hynes RO. Central roles of alpha5beta1 integrin and fibronectin in vascular development in mouse embryos and embryoid bodies. *Arterioscler Thromb Vasc Biol*. 2002;22:927-933.
7. George EL, Baldwin HS, Hynes RO. Fibronectins are essential for heart and blood vessel morphogenesis but are dispensable for initial specification of precursor cells. *Blood*. 1997;90:3073-3081.
8. Shalaby F, Rossant J, Yamaguchi TP, Gertsenstein M, Wu XF, Breitman ML, Schuh AC. Failure of blood-island formation and vasculogenesis in Flk-1-deficient mice. *Nature*. 1995;376:62-66.
9. Yang JT, Rayburn H, Hynes RO. Embryonic mesodermal defects in alpha 5 integrin-deficient mice. *Development*. 1993;119:1093-1105.
10. Davis GE, Senger DR. Endothelial extracellular matrix: biosynthesis, remodeling, and functions during vascular morphogenesis and neovessel stabilization. *Circ Res*. 2005;97:1093-1107.
11. Folkman J, Shing Y. Angiogenesis. *J Biol Chem*. 1992;267:10931-10934.
12. Yamada KM, Even-Ram S. Integrin regulation of growth factor receptors. *Nat Cell Biol*. 2002;4:E75-E76.
13. Eliceiri BP. Integrin and growth factor receptor crosstalk. *Circ Res*. 2001;89:1104-1110.
14. Miyamoto S, Teramoto H, Gutkind JS, Yamada KM. Integrins can collaborate with growth factors for phosphorylation of receptor tyrosine kinases and MAP kinase activation: roles of integrin aggregation and occupancy of receptors. *J Cell Biol*. 1996;135:1633-1642.
15. Schwartz MA, Ginsberg MH. Networks and crosstalk: integrin signalling spreads. *Nat Cell Biol*. 2002;4:E65-E68.
16. Sieg DJ, Hauck CR, Ilic D, Klingbeil CK, Schafer E, Damsky CH, Schlaepfer DD. Fak integrates growth-factor and integrin signals to promote cell migration. *Nature Cell Biology*. 2000;2:249-256.
17. Wang JF, Zhang XF, Groopman JE. Stimulation of beta 1 integrin induces tyrosine phosphorylation of vascular endothelial growth factor receptor-3 and modulates cell migration. *J Biol Chem*. 2001;276:41950-41957.
18. Moro L, Venturino M, Bozzo C, Silengo L, Altruda F, Beguinot L, Tarone G, Defilippi P. Integrins induce activation of EGF receptor: role in MAP kinase induction and adhesion-dependent cell survival. *EMBO J*. 1998;17:6622-6632.
19. Podar K, Tai Y, Lin BK, Narisimhan RP, Sattler M, Kijima T, Salgia R, Gupta D, Chauhan D, Anderson KC. Vascular endothelial growth factor-induced migration of multiple myeloma cells is associated with b1 integrin- and phosphatidylinositol 3-kinase-dependent PKCA activation. *J Biol Chem*. 2002;277:7875-7881.
20. De S, Razorenova O, McCabe NP, O'Toole T, Qin J, Byzova TV. VEGF-integrin interplay controls tumor growth and vascularization. *Proc Natl Acad Sci U S A*. 2005;102:7589-7594.
21. Byzova TV, Goldman CK, Pampori N, Thomas KA, Bett A, Shattil SJ, Plow EF. A mechanism for modulation of cellular responses to VEGF: activation of the integrins. *Mol Cell*. 2000;6:851-860.
22. Wijelath ES, Murray J, Rahman S, Patel Y, Ishida A, Strand K, Aziz S, Cardona C, Hammond WP, Savidge GF, Rafii S, Sobel M. Novel vascular endothelial growth factor binding domains of fibronectin enhance vascular endothelial growth factor biological activity. *Circ Res*. 2002;91:25-31.
23. Wijelath ES, Rahman S, Murray J, Patel Y, Savidge G, Sobel M. Fibronectin promotes VEGF-induced CD34 cell differentiation into endothelial cells. *J Vasc Surg*. 2004;39:655-660.
24. Barkalow FJ, Schwarzbauer JE. Localization of the major heparin-binding site in fibronectin. *J Biol Chem*. 1991;266:7812-7818.
25. Kimizuka F, Taguchi Y, Ohdate Y, Kawase Y, Shimojo T, Hashino K, Kato I, Sekiguchi K, Titani K. Production and characterization of functional domains of human fibronectin expressed in *Escherichia coli*. *J Biochem (Tokyo)*. 1991;110:284-291.
26. Mostafavi-Pour Z, Askari JA, Whittard JD, Humphries MJ. Identification of a novel heparin-binding site in the alternatively spliced IIICS region of fibronectin: roles of integrins and proteoglycans in cell adhesion to fibronectin splice variants. *Matrix Biol*. 2001;20:63-73.
27. Ishida A, Murray J, Saito Y, Kanthou C, Benzakour O, Shibuya M, Wijelath ES. Expression of vascular endothelial growth factor receptors in smooth muscle cells. *J Cell Physiol*. 2001;188:359-368.
28. Nishibe T, Parry G, Ishida A, Aziz S, Murray J, Patel Y, Rahman S, Strand K, Saito K, Saito Y, Hammond WP, Savidge GF, Mackman N, Wijelath ES. Oncostatin M promotes biphasic tissue factor expression in smooth muscle cells: evidence for Erk-1/2 activation. *Blood*. 2001;97:692-699.
29. Suda Y, Arano A, Fukui Y, Koshida S, Wakao M, Nishimura T, Kusumoto S, Sobel M. Immobilization and clustering of structurally defined oligosaccharides for sugar chips: an improved method for surface plasmon resonance analysis of protein-carbohydrate interactions. *Bioconjugate Chem*. 2006. In press.
30. Lyon M, Rushton G, Askari J, Humphries M, Gallagher J. Elucidation of the structural features of heparan sulfate important for interaction with the hep-2 domain of fibronectin. *J Biol Chem*. 2000;275:4599-4606.
31. Sobel M, Soler DF, Kermod JC, Harris RB. Localization and characterization of a heparin binding domain peptide of human von Willebrand factor. *J Biol Chem*. 1992;267:8857-8862.
32. Woods A, McCarthy JB, Furcht LT, Couchman JR. A synthetic peptide from the COOH-terminal heparin-binding domain of fibronectin promotes focal adhesion formation. *Mol Biol Cell*. 1993;4:605-613.
33. Chon JH, Chaikof EL. A von Willebrand factor-derived heparin-binding peptide regulates cell-substrate adhesive strength and chemokinesis behavior. *Biochim Biophys Acta*. 2002;1542:195-208.
34. Soldi R, Mitola S, Strasly M, Defilippi P, Tarone G, Bussolino F. Role of alphavbeta3 integrin in the activation of vascular endothelial growth factor receptor-2. *EMBO J*. 1999;18:882-892.
35. Rahman S, Patel Y, Murray J, Patel KV, Sumathipala R, Sobel M, Wijelath ES. Novel hepatocyte growth factor (HGF) binding domains on fibronectin and vitronectin coordinate a distinct and amplified Met-integrin induced signalling pathway in endothelial cells. *BMC Cell Biol*. 2005;6:8.
36. Kisucka J, Butterfield CE, Duda DG, Eichenberger SC, Saffaripour S, Ware J, Ruggeri ZM, Jain RK, Folkman J, Wagner DD. Platelets and platelet adhesion support angiogenesis while preventing excessive hemorrhage. *Proc Natl Acad Sci U S A*. 2006;103:855-860.
37. Hynes RO. A reevaluation of integrins as regulators of angiogenesis. *Nat Med*. 2002;8:918-921.
38. Taverna D, Hynes RO. Reduced blood vessel formation and tumor growth in alpha5-integrin-negative teratocarcinomas and embryoid bodies. *Cancer Res*. 2001;61:5255-5261.
39. Sahni A, Khorana AA, Baggs RB, Peng H, Francis CW. FGF-2 binding to fibrin(ogen) is required for augmented angiogenesis. *Blood*. 2006;107:126-131.

# Immobilization and Clustering of Structurally Defined Oligosaccharides for Sugar Chips: An Improved Method for Surface Plasmon Resonance Analysis of Protein–Carbohydrate Interactions

Yasuo Suda,<sup>\*,†,‡</sup> Akio Arano,<sup>‡</sup> Yasuhiro Fukui,<sup>§</sup> Shuhei Koshida,<sup>§</sup> Masahiro Wakao,<sup>†</sup> Tomoaki Nishimura,<sup>†,‡</sup> Shoichi Kusumoto,<sup>§,∇</sup> and Michael Sobel<sup>‡</sup>

Department of Nanostructure and Advanced Materials, Graduate School of Science and Engineering and Venture Business Laboratory, Kagoshima University, Kohrimoto, Kagoshima 890-0065, Japan, Japan Science and Technology Agency (JST), 5-3-4 Bancho, Chiyoda-ku, Tokyo 102-8666, Japan, Department of Chemistry, Graduate School of Science, Osaka University, Toyonaka, Osaka 560-0043, Japan, and Department of Surgery, University of Washington and VA Puget Sound Health Care System, Seattle, Washington 98108. Received March 11, 2006; Revised Manuscript Received July 7, 2006

Oligosaccharides are increasingly being recognized as important partners in receptor–ligand binding and cellular signaling. Surface plasmon resonance (SPR) is a very powerful tool for the real-time study of the specific interactions between biological molecules. We report here an advanced method for the immobilization of oligosaccharides in clustered structures for SPR and their application to the analysis of heparin–protein interactions. Reductive amination reactions and linker molecules were designed and optimized. Using mono-, tri-, or tetravalent linker compounds, we incorporated synthetic structurally defined disaccharide units of heparin and immobilized them as ligands for SPR. Their binding to an important hemostatic protein, von Willebrand factor (vWf), and its known heparin-binding domain was quantitatively analyzed. These multivalent ligand conjugates exhibited reproducible binding behavior, with consistency of the surface conditions of the SPR chip. This novel technique for oligosaccharide immobilization in SPR studies is accurate, specific, and easily applicable to both synthetic and naturally derived oligosaccharides.

## INTRODUCTION

Oligosaccharides of two to ten sugar moieties are responsible for many important biological functions (1). Both the specific structural attributes of the minimum oligosaccharide unit and the spacing and distribution of these key binding units determine the ultimate biological function of heparins and heparin-like glycosaminoglycans (2). Often, the minimal oligosaccharide unit with a structurally specific interaction may be as small as a di- or trisaccharide (3, 4). However, for full biological activity, these key binding units must often be presented in repeating units or clusters, appropriately spaced to interact with the heparin-binding sites of the cognate protein. Two major problems arise in the study of these structure–function relations. First, it is not easy to obtain large quantities of a homogeneous, structurally defined oligosaccharide. They cannot be expressed recombinantly, like proteins, and therefore, long and tedious chemical processes are necessary to synthesize or derive them from natural sources. The second problem is that an individual oligosaccharide motif may have low affinity but in biological systems they are often presented in clustered or repeating forms, which contribute significantly to their potency and affinity. We hypothesized that a chip or an array technology, in which structurally defined key oligosaccharide binding units are two-dimensionally immobilized on a surface, would be an effective

method to solve these problems and could be used as a high-throughput screening method.

A number of investigators have tackled the challenges of oligosaccharide immobilization. Techniques for self-assembled monolayers have been described by Horan et al. (5), Mirksich and co-workers (6, 7), and others. However, no method has so far been devised that both is procedurally simple and does not significantly modify or potentially interfere with the biological activity of the oligosaccharide. Most of these techniques require significant chemical modifications of the glycans, potentially obscuring the interpretation of structure–function relations. For example, conventional methods have involved chemical modifications at the 1-position of the carbohydrate, such as amination or allylation (8, 9). But these approaches invariably put functional sulfate or phosphate groups at risk. Finally, currently established methods do not afford the opportunity to control the clustering or multimerization of oligosaccharide functional domains. To this end, we pursued novel immobilization strategies for oligosaccharides, which would be technically simpler and less destructive, making them useful to a wider group of investigators. For detection, we chose surface plasmon resonance (SPR) technology, which permits the real-time analysis of molecular binding using microgram quantities of analyzing materials, without further labeling (10–14). It can measure the binding affinity and on (association) and off (dissociation) rates and is useful for high-throughput screening of new drug targets.

In previous work, we had shown that a specific disaccharide unit in heparin, *O*-(2-deoxy-2-sulfamido-6-*O*-sulfo- $\alpha$ -D-glucopyranosyl)-(1-4)-2-*O*-sulfo- $\alpha$ -L-idopyranosyluronic acid (abbreviated as GlcNS6S-IdoA2S), was a key unit responsible for heparin binding to human platelets (15) and von Willebrand factor (vWf) (16). We also found that the clustering of these disaccharides significantly enhanced the interaction (17, 18). To systematically investigate heparin's binding interactions, we

\* Corresponding author. Tel: +81-99-285-8369 or +81-99-285-8598. Fax: +81-99-285-3630. E-mail: ysuda@eng.kagoshima-u.ac.jp.

<sup>†</sup> Kagoshima University.

<sup>‡</sup> Japan Science and Technology Agency.

<sup>§</sup> Osaka University.

<sup>∇</sup> Present address: Suntory Institute for Bioorganic Research, Shimamoto-cho, Mishima-gun, Osaka 618-8503, Japan.

<sup>‡</sup> University of Washington and VA Puget Sound Health Care System.